Electroless copper-based layers deposition on anodized aluminum

V. S. Milusheva *[1,2], B. R. Tzaneva [1], M. Chr. Petrova [2], B. I. Stefanov[1]

[1]*Department of Chemistry, Technical University of Sofia, 8 Kliment Ohridski Blvd., 1000 Sofia, Bulgaria*
[2]*Department of Electrochemistry and Corrosion, Institute of Physical Chemistry-Bulgarian Academy of Science, Acad. G. Bonchev Str., Blok 11, 1113 Sofia, Bulgaria*

This work is an investigation on neutral electrolytes for electroless copper and copper (I) oxide plating of anodized aluminum. The plating electrolytes were based on copper (II) sulfate and phosphorous acid (H_3PO_3) as a reducing agent. It was investigated the influence of factors, such as Cu^{2+} concentration (0.024 – 0.048 mol/L) and pH (5 – 8) of the copper plating bath on the thickness, morphology and phase composition of the coatings, as well as kinetics of the electroless coating growth. The thickness and deposition rates of the coatings were determined gravimetrically and by X-ray fluorescence analysis. Electroless layer morphology was studied by optical and scanning electron microscopy. Crystallographic information and element composition depth profiles were examined by XRD and EDX analyzes respectively. Optimal deposition rates were achieved with electrolytes with Cu^{2+} concentration of 0.04 mol/L. Metallic copper layers were only formed at pH 5, while copper (I) oxide (Cu_2O) was formed at higher pH and the underlying mechanism was proposed.

INTRODUCTION

Anodic aluminum oxide (AAO) has a variety of applications, e.g. in optics and electronic industry, where it is used as a dielectric layer in printed circuit boards (PCB) manufacturing. In this particular application it is also needed to create electrically conductive (usually copper-based) or semiconducting layers on the AAO surface [1-5]. Typically, this is achieved through vacuum technology, such as chemical or physical vapor deposition methods (CVD, PVD). These approaches, however, require expensive equipment and produce relative thin layers. An alternative approach allowing for fast deposition of metallic layers on dielectric surfaces is electroless deposition. This method has a number of advantages over vacuum methods. It is inexpensive and requires simpler equipment; allows for deposition on both conductive and non-conductive substrates; and uniform layers are obtained regardless of surface profile [6].

The electroless copper plating bath has two main components – a copper salt and a suitable reducing agent. Conventional electrolytes for electroless copper deposition, however, can be aggressive towards AAO, which is unstable in highly acidic or alkaline solutions, as well as when chloride ions are present in the solution [7]. Usually formaldehyde, or formaldehyde-based derivatives, are used as a reducing agent for copper deposition [8, 9] and copper (I) oxide [10, 11], in order to achieve fast deposition rates and good mechanical stability of the as-prepared coatings. The catalytic oxidation rate of formaldehyde increases with hydroxide concentration and is most effective at pH > 11, thus making formaldehyde-based deposition chemistry unsuitable for metallization of AAO. There are a few examples of neutral electroless copper deposition electrolytes in the literature, which are still not used in practical applications [12, 13].

In this paper we present a novel electrolyte suitable for electroless copper deposition on AAO, employing phosphorous acid (H_3PO_3) as a reducing agent. Main focus of the study was investigating the effects of pH and Cu^{2+} ion concentrations on

the deposition rate and morphology of the electroless deposited layers onto the AAO surface. This is a continuation of previous studies done in our group, where weakly alkaline electroless copper plating baths, based on sodium hypophosphite were employed on ABS and AAO substrates [14]. In this case it was observed the formation of copper (I) oxide on the AAO surface.

Copper (I) oxide (cuprous oxide, Cu_2O) is a n-type semiconductor with unique optical and electrical properties, which finds promising applications for solar energy conversion, photocatalytic oxidation, catalysis and sensors [15, 16]. It can also easily react with oxygen in moist atmosphere which implies promising applications in electrocatalytic applications, such as ORR [17, 18]. Yan et al [17] also show that the electrical conductivity of Cu_2O nanoparticles can be improved by the addition of highly conductive carbon-based materials, such as graphene.

EXPERIMENTAL

AAO samples 20x10 mm in dimensions were prepared by anodization of 100 μm thick Al-foil (99.0% purity). Prior anodization it was treated in 40 g/L NaOH solution. Anodization was carried using 20% H_2SO_4 electrolyte and a Voltcraft®4050 potentiostat set to 20V and current density up to 10 mA/cm^2. Temperature was set to 15 ºC and the duration of anodization was 100 min, resulting in an anodized layer of 12 μm. Active sites catalysing the electroless Cu deposition were created on the AAO surface by soaking the samples in Pd^{2+} solution.

The electrolytes for electroless copper deposition were based on phosphorous acid reducing agent and Cu^{2+} copper precursor salt. To study effects of Cu^{2+} concentration it was varied in the range 0.024 – 0.048 mol/L. The effect of pH was studied by adjusting the pH of the electrolyte in the range 5.0 – 8.0 with 10M NaOH. Details about the electrolyte composition and deposition conditions are listed in Table 1.

Copper-based coating thickness was determined employing X-Ray Fluorescence (XRF - Fischerscope HDAL) analysis and is noted as h_{XRF}. The obtained XRF results were compared with those determined

Table 1: Composition of electroless plating bath and summary of operating conditions for deposition on AAO

Substances	Concentration (mol/L)
$CuSO_4.5H_2O$	0.024 – 0.048
$H_3PO_3.H_2O$	0.33 – 0.6
$Na_3C_6H_5O_7.5,5H_2O$	0.058 – 0.1
H_3BO_3	0.56 – 1.00
Operation conditions	
pH	5.0 – 8.0
Temperature, ˚C	60

gravimetrically (h_{grav}) by weighing measurement the samples before and after the electroless deposition on an analytical scale (0.1 mg precision) and using Eq.1:

$$h_{grav} = \frac{\Delta m}{D.S} \qquad (1)$$

where Δm is the increase of samples mass due to the copper-based layer; D is the density of copper (8.96 g/cm^3) or of copper (I) oxide (6.0 g/cm^3); and S is the geometric area of the samples (4 cm^2).

Surface morphology of the copper-based layers was determined via optical microscopy (Optika XDS-3MET) and scanning electron microscopy (SEM, JEOL JSM 733) equipped with EDS detector (INKA). Crystallographic information was obtained by X-Ray Diffraction (XRD, PANanalytical Empyrean, Pixel 3D multichannel detector at Cu Kα) and diffractograms were obtained in the 10-100° 2θ range, 0.01° resolution.

RESSULTS AND DISCUSION

Influence of Cu^{2+} concentration on electroless deposition rates

The influence of increasing the Cu^{2+} concentration in the electroless deposition electrolytes is summarized as layer thickness values listed Table 2 (for 60 ºC and pH 6.5). Data is presented for samples, where the deposition time was limited to 20 min. In the range 0.027 – 0.035 mol/L the XRF determined thickness increases linearly in the range 0.393 – 0.486 μm, which is the highest achievable thickness at these conditions. Increasing the Cu^{2+} concentration past 0.035 mol/L, and up to 0.048 mol/L, does not affect the kinetics of electroless deposition.

Optical microscopy observation of the electroless coated samples at x500

magnification show that at lower Cu^{2+} concentrations (0.027 mol/L) uneven coatings with uncoated areas were observed, while increasing the concentration to 0.035 mol/L the AAO surface was evenly coated within the same duration of electroless deposition (20 min). An attempt to improve the uniformity of the copper-based coating at lower Cu^{2+} concentrations (0.024 mol/L) was made by increasing the deposition bath temperature from 60 ℃ to 70 ℃. In this case visible copper layer were obtained; however, the rate of deposition was unsatisfactory with only 0.2 μm being deposited within 1h (determined by XRF). Thus, it can be concluded that Cu^{2+} affects deposition rates more than temperature and the optimal conditions for electroless copper deposition in our case are: 60 ℃ and 0.04 mol/L Cu^{2+} concentration in the electrolyte.

Table 2. Thickness of the electroless copper-based layer (determined gravimetrically or via XRF), obtained for 20 min deposition time (pH 6.5, 60 ℃) for several Cu^{2+} concentrations

Cu^{2+}, mol/L	0.027	0.030	0.035	0.040	0.048
$h_{grav.}$, μm	0.573	0.597	0.689	0.687	0.691
h_{XRF}, μm	0.393	0.424	0.486	0.436	0.449

Influence of pH on electroless deposition rates

The influence of pH of the electrolyte on the copper-based layer thickness and on the deposition rate was studied by comparing results at pH 5, pH 6.5 and pH 8 with a Cu^{2+} concentration of 0.04 mol/L. The results are summarized in Table 3 and Fig. 1 respectively.

Table 3. Time-dependence of the electroless Cu-based layer thickness (determined gravimetrically or via XRF) for different electroless copper plating bath pH

Time of deposition, min		5	10	20	30	60
pH=5.0	h_{XRF}, μm	0.055	0.069	0.154	0.105	0.067
pH=6.5	$h_{grav.}$, μm	0.303	0.585	0.687	1.250	1.476
	h_{XRF}, μm	0.167	0.310	0.451	0.619	0.955
pH=8.0	h_{XRF}, μm	0.112	0.134	0.157	0.165	0.186
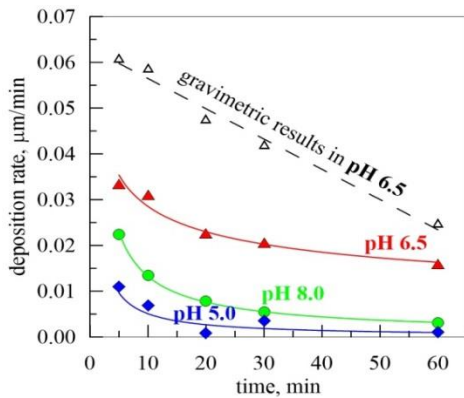
Fig. 1. Time-dependence of the deposition rate of the electroless copper-based layer (0.04 mol/L Cu^{2+}, pH 6.5, 60 ℃) at pH 5.0, 6.5, and 8.5. As obtained by XRF (solid lines) and gravimetric (dashed line).

Visible layers with various colour were observed in all three cases, however, both increasing and decreasing the pH had a detrimental effect on its deposition rate. A maximum thickness of 1 μm was obtained in electrolyte with pH 6.5 after 60 min of

deposition. Thus, pH 6.5 was found to be the optimal condition.

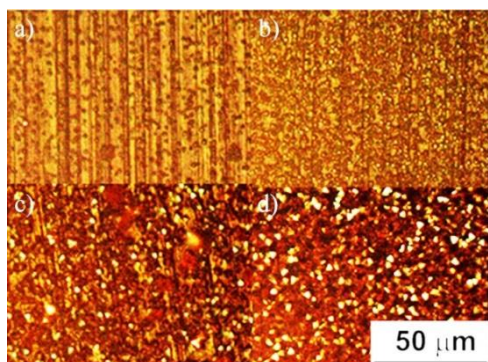According to XRF thickness results the rate deposition decrease flowing a power equation: $\ln(rate) = a + b.\ln(time)$

It can be observed that the copper-based layer grows rapidly during the first minutes of deposition, which is followed by a rapid decrease in deposition rate.

Morphology, composition and structure of deposited electroless copper layer

Figure 2 presents optical micrographs of the electroless deposited layers taken after 5, 10, 30, and 60 min. During the first 5 min finely dispersed crystalline nuclei were formed (Fig. 2a) with their density being the highest around irregularities and deep crevices on the anodized aluminum surface. This can be explained by a higher concentration of Pd-catalytic centers around these surface features and respectively higher rates of electroless deposition of

copper there. The number of copper nucleation sites increases during the first 10 min until the entire surface is coated, however their size remains constant until then (Fig. 2b). Crystalline growth of the copper nuclei is only observed after the surface is completely coated – then visible 3D crystals can be registered (Fig. 2c). This observation implies that the Pd catalytic centers exhibit higher activation to the phosphorous acid oxidation, compared to the autocatalytic effect on the reaction by the deposited copper-based layers. It also confirms our observation that the copper deposition rate progressively decreases proportionally with the area of uncoated AAO surface and inversely with increasing the amount of deposited crystals. After 1h, the AAO surface is completely coated with pyramidally shaped red-orange crystals. The initial morphology of the Al-foil surface, preserved after anodization, is still visible during the first 5 min, however it is completely masked by the electroless deposited layer afterwards. It can be concluded that the electroless copper-based deposition at pH 6.5 is completed in two stages – the first step being the formation of Cu nucleus on Pd catalytic centers and then – their growth after the catalytic surface is completely covered in copper compounds.

structure and relatively narrow size distribution 2÷4 μm, completely coating the AAO surface. The size uniformity of the features of the electroless-deposited layer confirms our expectations that the growth mechanism consists of two stages, as described in the paragraph above.

EDX data obtained at two points across the copper coating cross-section (Fig. 3b) shows that copper completely penetrates the AAO layer down to the pores bottom. The results for elemental composition measured by EDX throughout the entire 12 μm AAO pore depth are presented in Fig. 3b in wt.%. Negligible amounts of phosphorus (0.15 wt.%) was detected only in one of EDX measurements and suggests that its presence is only due to surface adsorption of the reducing agent (H_3PO_3), rather than chemical binding inside the copper layer during its deposition.
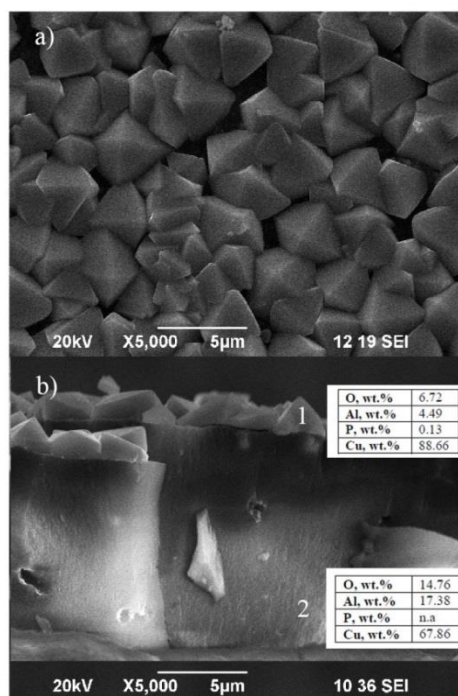
Fig. 3. SEM images of electroless deposited copper (I) oxide on AAO for 30 min at pH 6.5: (a) top and (b) cross-section view.

Fig. 2. Optical micrographs of electroless plated AAO (0.04 mol/L Cu^{2+}, pH 6.5, 60ºC) at different time-frame, a) 5 min; b) 10 min; c) 30 min; d) 60 min

Figure 3 shows SEM micrographs of the surface morphology and cross-section of AAO after electroless deposition for 30 min (0.04 mol/L Cu^{2+}, pH 6.5). It can be seen clearly that the deposited layer consists of densely packed crystals with pyramidal

Figure 4 shows XRD diffraction patterns of electroless deposited layers by the Cu^{2+}/H_3PO_3 electrolyte at pH 5, 6.5, and 8. Metallic copper was only formed at pH 5, as shown by its characteristic diffraction peaks at 2θ 43.3°, 50.3°, and 74.2°. The peaks are
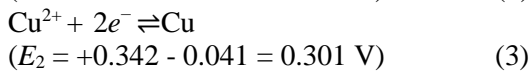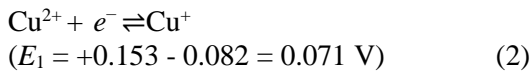
very weak and indicative of cubic copper crystals in various crystallographic orientations [18].
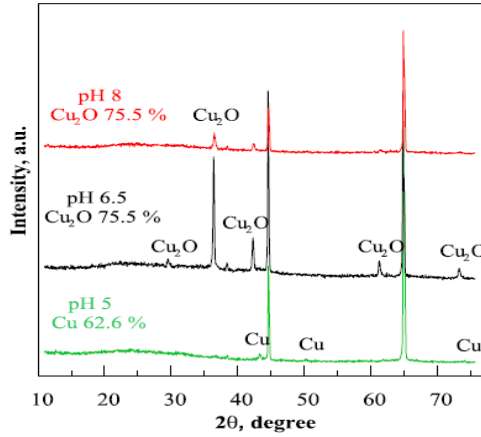

Fig. 4. XRD pattern of electroless copper-based layers grown on anodic aluminum oxide at pH 5.0, 6.5 and 8.0

At higher pH 6.5 and 8.0 new diffraction peaks are observed at 2θ 29.6°, 36.6°, 42.3°, 61.3° and 73.5°, which suggest the formation of Cu_2O. Similar results are found in the literature. According to Kobayashi et al [19] these peaks correspond to cubic Cu_2O. The highest intensity of the Cu_2O peaks is obtained at pH 6.5, suggesting also highest crystallinity at this condition. Therefore, in tables 2 and 3 the thickness of the deposited layers at pH 6.5 was calculated gravimetrically h_{grav} considering only the presence of copper (I) oxide.

At Cu^{2+} concentration of 0.04 mol/L, which was determined to be optimal for the highest rate of electroless layer deposition the reduction potentials for Cu^{2+} should be more negative than [20]:

$Cu^{2+} + e^- \rightleftharpoons Cu^+$
$(E_1 = +0.153 - 0.082 = 0.071 \text{ V})$ (2)
$Cu^{2+} + 2e^- \rightleftharpoons Cu$
$(E_2 = +0.342 - 0.041 = 0.301 \text{ V})$ (3)

The oxidation potential of phosphorous acid (H_3PO_3) to phosphoric acid (H_3PO_4) is pH dependent [21]:

$H_3PO_3 + H_2O - 2e^- \rightleftharpoons H_3PO_4 + 2H^+$
$(E = -0.276 - 0.059pH)$ (4)
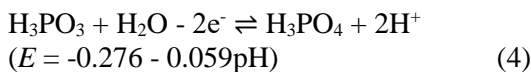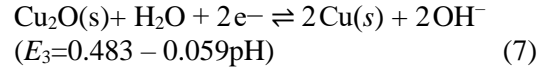
While sufficient to reduce Cu^{2+} through both pathways, (2) and (3), the complete reduction should be favoured, however, it is only observed at pH 5 in our experiments. Nevertheless, according to the Pourbaix

diagram of the process, when pH > 5 the Cu_2O formation reaction will be favoured. Hence, we can assume that the reduction of Cu^{2+} by H_3PO_3 goes according to the following two-step mechanism:

$Cu^{2+} + H_3PO_3 + 2H_2O \rightarrow Cu_2O + H_3PO_4 + 4H^+$ (5)

$Cu_2O + H_3PO_3 \rightarrow 2Cu + H_3PO_4$ (6)
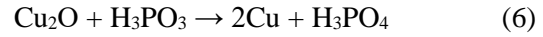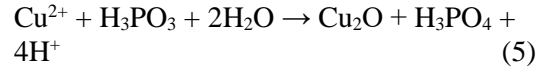
In the pH interval 5 – 12 the reduction potential for Cu_2O/Cu is:

$Cu_2O(s) + H_2O + 2e^- \rightleftharpoons 2Cu(s) + 2OH^-$
$(E_3=0.483 - 0.059pH)$ (7)

It is also pH dependent and the slope of the equation (7) is the same as the one for the H_3PO_3 oxidation (equation 4). Therefore, at pH 6.5 the reduction potential of Cu_2O and the oxidation potential of H_3PO_3 are 0.0997 and -0.6595 V vs. SHE, respectively. XRD data, however, suggests that reaction (6) has a negligible yield in our case and the process stops at Cu_2O.

According to Zhang et al [21] the morphology of the Cu_2O layer prepared by electroless deposition is determined by the deposition bath temperature. At 50 °C octahedral crystals are observed ca. 110 nm in diameter. In their publication TEM analysis is also made showing crystallographic growth favouring the formation of {111} facets [22].

CONCLUSIONS

We present a study on the electroless deposition of copper–based layers onto anodic aluminium oxide (AAO) surface. The deposition was achieved by using pH neutral electrolyte (pH 5 – 8) compatible with AAO. The effect of pH and Cu^{2+} ion concentrations was investigated in order to achieve optimal deposition rates and phase composition. The optimal deposition rate was achieved at Cu^{2+} concentration of 0.04 mol/L, pH 6.5, and 60°C temperature, where uniform cubic copper (I) oxide crystals were obtained on the entire surface of the AAO substrate. It was found that adjusting the pH affects the phase composition of the deposited copper layer, leading to formation of metallic copper at pH 5 and predominantly Cu_2O at pH > 5.

REFERENCES

1. Ch.-W. Hsu, Zh.-D. Chou, and G.-J. Wang, *J. Microelectromechanical systems,* **19,** 849 (2010).
2. S. Thongmee, H.L. Pang, J. Ding, J.B. Yi, J.Y. Lin, Proc 2th IEEE International Nanoelectronics Conference (INEC 2008) (2008), p.1116.
3. J. Cui, Y. Wu, Y. Wang, H. Zheng, G. Xu, X. Zhang, *Appl. Surf. Sci*., **258,** 5305 (2012).
4. G.D. Sulka, A. Brzozka, L. Zaraska, M. Jaskula, *Electrochim. Acta,* **55,** 4368 (2010).
5. Ch. Hong, L. Chu, W. Lai, A.-Sh. Chiang, W. Fang, *IEEE Sensors journal*, **11**, 3409 (2011).
6. Ch. Decker, *Plating & Surface Finishing*, **82**, 48 (1995).
7. B.R. Tzaneva*, Bulg. J. Chem.* **2,** 61 (2013).
8. M. Georgieva, G. Avdeev, D. Stoychev, M. Petrova, *Transactions of the IMF*, **93**, 97 (2015).
9. S. Nakahara, Y. Okinaka, H. Straschil, *J. Electrochem. Soc*., **136**, 1120 (1989).
10. K. Phasuksom, W. Prissanaroon-Ouajai, N. Brack, P. Pigram, *Adv. Mater. Research*, **802**, 262 (2013).
11. M.D. Susman, Y. Feldman, A. Vaskevich, I. Rubinstein, *ACS Nano,* **8**, 162 (2014).
12. Q. Li, P. Xu, B. Zhang, H. Tsai, S. Zheng, G. Wu, H.L. Wang, *J. Phys. Chem. C*, **117**, 13872 (2013).
13. F. Matsui, Y. Yamamoto, *US Patent* 5 298 058 (1994).
14. V. Milusheva, M. Georgieva, B. Tzaneva, M. Petrova, Proc. of IEEE XXVII International Scientific Conference Electronics - ET, Sozopol, Bulgaria, 2018, p. 1 (DOI 10.1109/ET.2018.8549651).
15. M. Wang, J. Huang, Z. Tong, W. Li, J. Chen, *J. Alloys Compd,* **568**, 26 (2013).
16. S. Deng, V. Tjoa, H.M. Fan, H.R. Tan, D.C. Sayle, M. Olivo, S. Mhaisalkar, J. Wei, C.H. Sow, *J. Am. Chem. Soc*., **134**, 4905 (2012).
17. X. Y. Yan, X. L. Tong, Y. F. Zhang, X. D. Han, Y. Y. Wang, G. Q. Jin, Y. Qin, X. Y. Guo, *Chem. Commun.*, **48**, 1892 (2012).
18. JCPDS: 4-0836
19 Y. Kobayashi, Y. Abe, T. Maeda, Y. Yasuda, T. Morita, *J. Mater. Res. Technol.,* **3**, 114 (2014).
20. P. Vanýsek "Electrochemical Series" in: Chemistry and Physics: 93rd Edition, W.M. Haynes (ed.), CRC press, Taylor&Francis Group, New York, 2012, p. 5.
21. N. Koura, in: Electroless Plating: Fundamentals and Appications: G. O. Mallory, J. B. Hajdu (eds.), William Andrew, Orlando,1990, p. 448.
22. X. Zhang, Y. Zhang, H. Huang, J. Cai, K. Ding, S. Lin, *New Journal of Chemistry*, **42**, 458 (2018).